

## Intraband transitions in magnetoexcitons in coupled double quantum wells

A. B. Dzyubenko\*)

*Institute of General Physics, Russian Academy of Sciences, 117942 Moscow, Russia;  
Walter Schottky Institute, Technische Universität München, D-85748 Garching, Germany  
(Submitted 8 October 1997)*

Zh. Éksp. Teor. Fiz. **113**, 1446–1459 (April 1998)

A theory of far-infrared (FIR) magneto-optical intraband  $s \rightarrow p^\pm$  transitions of direct and indirect excitons in semiconductor coupled double quantum wells has been developed. The case of symmetric strained  $\text{In}_x\text{Ga}_{1-x}\text{As}/\text{GaAs}$  quantum wells with nondegenerate valence band in the regime of both narrow and wide barriers has been analyzed. The energies and dipole matrix elements of transitions between the ground  $s$  and excited  $p^\pm$  states in a quantizing magnetic field  $B > 2$  T and electric field  $\mathcal{E}$  perpendicular to the quantum well plane have been studied. The regimes of direct (in a weak electric field) and indirect (in a strong electric field) transitions, and the transition between the direct and indirect regimes, have been investigated.

© 1998 American Institute of Physics. [S1063-7761(98)02304-X]

### 1. INTRODUCTION

Two-dimensional (2D) spatially separated electron–hole ( $e-h$ ) systems in a strong magnetic field have been studied theoretically for a number of years.<sup>1</sup> Depending on the separation  $d$  between  $e$ - and  $h$ -layers and the population number of excitons at the lowest Landau level,  $\nu_X = 2\pi l_B^2 n_X$  (where  $n_X$  is the exciton density and  $l_B = (\hbar c/eB)^{1/2}$ ), such systems demonstrate an abundance of possible low-temperature phases. In particular, at small  $d$  Bose–Einstein condensation of magnetoexcitons in the state with momentum  $K=0$  is possible (see also Ref. 2, where exact many-body results in the limit  $d=0$  were obtained).

In order to check theoretical predictions, real quasi-two-dimensional systems with sufficiently long exciton lifetimes are necessary. Recently experimenters' attention has been focused on systems of this kind.<sup>3–7</sup> Some evidence in favor of condensation of indirect excitons in a strong magnetic field was provided by interband magneto-optical spectroscopy (with a temporal and spatial resolution) of type II GaAs/AlAs quantum wells.<sup>3</sup> In addition, anomalies were detected in low-temperature transport properties of excitons in a magnetic field.<sup>8</sup> Other semiconductor structures that have been intensely studied in recent times are InGaAs/GaAs<sup>4</sup> and GaAs/GaAlAs<sup>5</sup> coupled double quantum wells (DQW). When an electric field  $\mathcal{E}$  is applied normally to the quantum well plane, the exciton ground state is modified (direct-to-indirect crossover). In a strong electric field  $\mathcal{E}$  the ground state is an indirect exciton (Fig. 1), whose radiative lifetime is considerably longer. This makes it possible to investigate many-body effects in neutral  $e-h$  systems in a strong magnetic field  $B$  at low exciton temperatures.

Identification of many-body effects in optical spectra demands detailed knowledge of optical properties of excitons in DQW in a strong magnetic field. The theory of magneto-optical transitions of excitons in InGaAs/GaAs DQW in a low-density regime was presented in our previous publication<sup>9</sup> and is in good agreement with experimental

data.<sup>4</sup> The intraband FIR magnetospectroscopy proved to be an efficient tool in studies of the ground and excited states of excitons in bulk indirect semiconductors (see Ref. 10 and references therein). Experimental results concerning quasi-two-dimensional excitons obtained by this technique began to emerge relatively recently. FIR magnetospectroscopy was used<sup>6</sup> in measurements of  $e-h$  interaction as a function of the population number in type II InAs/AlGaSb quantum wells. Evidence in favor of the existence of a stable exciton state in a strong magnetic field (in the presence of excess free electrons) was obtained.<sup>7</sup> FIR spectra of type II GaAs/AlAs quantum wells in a strong magnetic field were also measured in the regime of low exciton density.<sup>11</sup> Another highly sensitive technique, namely the optically detected cyclotron resonance, was used in studies of direct excitons in GaAs quantum wells.<sup>12–15</sup>

No detailed theoretical study of intraband magneto-optical properties of quasi-two-dimensional excitons has been published as yet. On the contrary, one can even find in the literature erroneous claims<sup>16</sup> about the energy of  $s \rightarrow p$  intraexciton transitions as a function of the magnetic field (a drop in the transition energy with  $B$ ), which contradict experimental data.<sup>15</sup> Previously we analyzed changes in the  $1s \rightarrow np^\pm$  transitions in DQW due to the magnetic field in the regime of a wide barrier between wells at  $\mathcal{E}=0$ .<sup>17</sup>

This paper reports on a theoretical investigation of the energies and dipole matrix elements of FIR transitions in symmetric InGaAs/GaAs DQW as functions of the barrier width in a strong magnetic field  $B=10$  T (Sec. 3.1), changes in the transitions caused by an applied electric field  $\mathcal{E}$  in a fixed magnetic field (Sec. 3.2), and changes in these parameters with a magnetic field under strong and intermediate electric fields  $\mathcal{E}$  (Sec. 2.1). Sections 2.1–2.3 describe the calculation techniques, and Sec. 2.4 gives a qualitative description of magnetoexciton spectra in DQW. Some results of this work were briefly reported in our previous publications.<sup>17,18</sup>

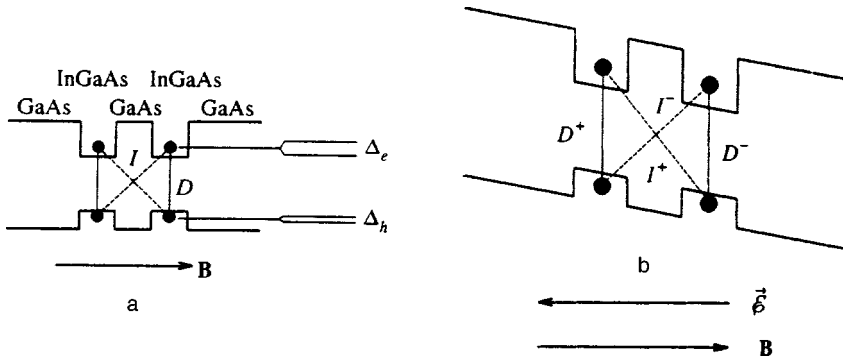


FIG. 1. a) Direct  $D$  and indirect  $I$  excitons in DQW. Splittings between symmetric and antisymmetric states of electrons and holes,  $\Delta_e$  and  $\Delta_h$ , are shown. b) Excitons in DQW in an electric field

## 2. THEORETICAL MODEL

### 2.1. System Hamiltonian

Consider a heavy-hole exciton in a symmetric strained  $\text{In}_{x_1}\text{Ga}_{1-x_1}\text{As}/\text{GaAs}/\text{In}_{x_2}\text{Ga}_{1-x_2}\text{As}$  DQW with  $x_1=x_2=0.2$ , well widths  $L_1=L_2$ , and barrier width  $L_b$  (Fig. 1). Light holes, whose branch is separated from that of heavy holes by several tens of meV, can be neglected.<sup>19</sup> The exciton Hamiltonian in DQW in perpendicular electric  $\mathcal{E}=(0,0,\mathcal{E})$  and magnetic  $\mathbf{B}=(0,0,B)$  fields can be expressed as

$$H = H_{ez} + H_{hz} + H_{2D} + U_{eh} \equiv H_0 + U_{eh}, \quad (1)$$

where the Hamiltonian components

$$H_{ez} = -\frac{\hbar^2}{2m_e} \frac{\partial^2}{\partial z_e^2} + V_e(z_e) + e\mathcal{E}z_e, \quad (2)$$

$$H_{hz} = -\frac{\hbar^2}{2m_{hz}} \frac{\partial^2}{\partial z_h^2} + V_h(z_h) - e\mathcal{E}z_h \quad (3)$$

describe the motion of free electrons and holes along the  $z$ -axis. The well depths for electrons and holes are assumed to be  $V_{ei}=0.8\Delta E_g(x_i)$  and  $V_{hi}=0.2\Delta E_g(x_i)$ , where  $\Delta E_g(x_i)=E_g(0)-E_g(x_i)$  is the band-gap offset,  $E_g(x)=1.519-1.47x+0.375x^2$  eV is the gap width in  $\text{In}_x\text{Ga}_{1-x}\text{As}$ , and the effective masses are  $m_e=0.067$  and  $m_h=0.35$ .<sup>9,19</sup> The exciton energy is measured with respect to  $E_g(0)$ .

The solutions of the one-dimensional Schrödinger equations

$$H_{ez}\zeta_i(z_e) = E_i^{(e)}\zeta_i(z_e), \quad H_{hz}\xi_j(z_h) = E_j^{(h)}\xi_j(z_h), \quad (4)$$

corresponding to the lowest discrete levels are calculated numerically. In order to avoid difficulties with the continuum in an electric field  $\mathcal{E} \neq 0$ , boundary conditions corresponding to infinite energy barriers at sufficient distances (200–500 Å) from the DQW are invoked. When  $\mathcal{E}=0$  and the DQW is symmetric (i.e., the two wells are identical at  $x_1=x_2$  and  $L_1=L_2$ ), the subscripts  $i, j=s, a$  correspond to the symmetric ground state ( $s$ ) and antisymmetric first excited state ( $a$ ) of electrons and holes, respectively:

$$\zeta_{s(a)}(z_e) = \pm \zeta_{s(a)}(-z_e), \quad \xi_{s(a)}(z_h) = \pm \xi_{s(a)}(-z_h). \quad (5)$$

The splittings between symmetric and antisymmetric states,  $\Delta_e = E_a^{(e)} - E_s^{(e)}$  and  $\Delta_h = E_a^{(h)} - E_s^{(h)}$ , are determined by penetration of the wave functions under the barrier (see Sec. 3.1).

The Hamiltonian  $H_{2D}$  of relative motion of a noninteracting electron-hole pair with magnetic momentum of the center of mass  $\mathbf{K}$  in a perpendicular magnetic field  $B$  has the form<sup>20,21</sup>

$$H_{2D} = -\frac{\hbar^2}{2\mu} \nabla_{\rho}^2 + \frac{1}{2} \hbar(\omega_{ch} - \omega_{ce}) \hat{l}_z + \frac{e^2 B^2}{8\mu c^2} \rho^2 + \frac{e}{Mc} \mathbf{B} \cdot (\boldsymbol{\rho} \times \mathbf{K}) + \frac{K^2}{2M}, \quad (6)$$

where  $\boldsymbol{\rho} = \boldsymbol{\rho}_e - \boldsymbol{\rho}_h$  is the relative separation,  $\mu^{-1} = m_e^{-1} + m_{h\parallel}^{-1}$  is the reduced mass,  $\omega_{ce(h)} = eB/m_{e(h)}c$  is the electron (hole) cyclotron frequency, and  $\hat{l}_z = -i(\boldsymbol{\rho} \times \nabla_{\rho})_z$  is the  $z$ -projection of the orbital angular momentum of relative motion. In this formula we have taken advantage of the existence of an exact integral of the motion, namely the magnetic center-of-mass momentum,<sup>20</sup> whose operator is

$$\hat{\mathbf{K}} = -i\hbar \nabla_{\mathbf{R}} - \frac{e}{c} \mathbf{A}(\boldsymbol{\rho}),$$

where  $\mathbf{R} = (m_e \boldsymbol{\rho}_e + m_{h\parallel} \boldsymbol{\rho}_h)/M$  is the center-of-mass location, and  $M = m_e + m_{h\parallel}$ . The vector potential is expressed in the symmetric gauge  $\mathbf{A} = \frac{1}{2} \mathbf{B} \times \boldsymbol{\rho}$ , and  $\mathbf{r} = (\boldsymbol{\rho}, z)$ . Note that in Eqs. (2), (3), and (6), an isotropic electron spectrum is assumed, while the masses of holes moving in the quantum well plane and in the perpendicular direction are different,  $m_{h\parallel} \neq m_{hz}$  (see Appendix to Ref. 9, where the nonparabolicity of  $m_{h\parallel}$  is discussed). In what follows, we will neglect the difference between effective masses in the InGaAs wells and GaAs barriers. The energy of the Coulomb interaction between electrons and holes can be written in the form

$$U_{eh} = U_{eh}(|\mathbf{r}_e - \mathbf{r}_h|) = -\frac{e^2}{\epsilon |\mathbf{r}_e - \mathbf{r}_h|}, \quad (7)$$

where  $\epsilon = 12.5$ . In a InGaAs/GaAs DQW, the effect of electrostatic image forces is very weak, owing to the small difference between the dielectric constants of GaAs ( $\epsilon = 12.5$ ) and  $\text{In}_{0.2}\text{Ga}_{0.8}\text{As}$  ( $\epsilon = 13$ ),<sup>9</sup> so this effect is neglected.

## 2.2. Wave functions of magnetoexcitons with $\mathbf{K}=0$

In order to calculate the eigenfunctions of Hamiltonian (1), we diagonalize the term  $U_{eh}$  of electron–hole interaction in the basis of the wave functions of noninteracting electron–hole pairs in a DQW in a magnetic  $B$  and electric  $\mathcal{E}$  fields. The wave function of an exciton with center-of-mass momentum  $\mathbf{K}=0$  (see Sec. 2.3) can be expressed in the form of the expansion<sup>9</sup>

$$\Psi_{\mathbf{K}=0, l_z}(\mathbf{r}_e, \mathbf{r}_h) = \exp\left(\frac{i[\boldsymbol{\rho} \times \mathbf{R}]_z}{2l_B^2}\right) \Phi_{l_z}(\boldsymbol{\rho}, z_e, z_h), \quad (8)$$

$$\Phi_{l_z}(\boldsymbol{\rho}, z_e, z_h) = \sum_{i,j=1,2} \sum_{n-m=l_z} A_{ijnm} \zeta_i(z_e) \xi_j(z_h) \phi_{nm}(\boldsymbol{\rho}), \quad (9)$$

where  $l_B = (\hbar c/eB)^{1/2}$ ,  $\zeta_i(z_e)$  and  $\xi_j(z_h)$  are the electron and hole wave functions determined by Eq. (4),  $\phi_{nm}(\boldsymbol{\rho}) = (a^\dagger)^n (b^\dagger)^m |00\rangle / \sqrt{n!m!}$  are the factored wave functions in a magnetic field  $B$ ,<sup>22,23</sup> and  $\boldsymbol{\rho} = \boldsymbol{\rho}_e - \boldsymbol{\rho}_h$ . For magnetoexcitons the quantum numbers  $n$  and  $m$  label the Landau levels of electrons and holes, respectively, and the angular momentum projection  $l_z = n - m$ . Note that the wave functions  $\phi_{nm}(\boldsymbol{\rho})$  of the  $e$ – $h$ -pairs correspond to bound states in a field  $B$  (the characteristic length scale  $\langle nm | \boldsymbol{\rho}^2 | nm \rangle = 2(n+m+1)l_B^2$ ). Therefore Eq. (9) can be considered an expansion in exciton wave functions. Note also that Eq. (9) takes into account mixing of different subbands  $i$  and  $j$ , which is important for accuracy of calculations (compare to the discussion in Ref. 24).

The energy eigenvalues  $E$  and eigenfunctions of Hamiltonian (1) for a magnetoexciton with angular momentum projection  $l_z = n - m$  are calculated by numerically solving the secular equation

$$\text{Det} \left( \left[ E_i^{(e)} + E_j^{(h)} + \hbar \omega_{ce} \left( n + \frac{1}{2} \right) + \hbar \omega_{ch} \left( m + \frac{1}{2} \right) - E \right] \right. \\ \left. \times \delta_{ii'} \delta_{jj'} \delta_{nn'} \delta_{mm'} + U_{ijnm}^{i'j'n'm'} \right) = 0, \quad (10)$$

where the matrix elements of the  $e$ – $h$  interaction have the form

$$U_{ijnm}^{i'j'n'm'} = \langle i'j'n'm' | U_{eh} | ijnm \rangle = \delta_{n'-m', n-m} \\ \times \int \frac{d^2q}{(2\pi)^2} \left( -\frac{2\pi e^2}{\varepsilon q} \right) F_{ij}^{i'j'}(q) \mathcal{D}_{nm}^{n'm'}(\mathbf{q}), \quad (11)$$

$$\delta_{n'-m', n-m} \mathcal{D}_{nm}^{n'm'}(\mathbf{q}) = \left( \frac{\min(n, n')! \min(m, m')!}{\max(n, n')! \max(m, m')!} \right)^{1/2} \\ \times \left( \frac{q^2 l_B^2}{2} \right)^{|n-n'|} L_{\min(n, n')}^{|n-n'|} \left( \frac{q^2 l_B^2}{2} \right) \\ \times L_{\min(m, m')}^{|m-m'|} \left( \frac{q^2 l_B^2}{2} \right) \exp\left( -\frac{q^2 l_B^2}{2} \right), \quad (12)$$

where  $L_n^m$  are the generalized Laguerre polynomials and

$$F_{ij}^{i'j'}(q) = \int_{-\infty}^{\infty} dz_e \int_{-\infty}^{\infty} dz_h \exp(-q|z_e - z_h|) \\ \times \zeta_i(z_e) \zeta_{i'}(z_e) \xi_j(z_h) \xi_{j'}(z_h) \quad (13)$$

are the form factors related to the wave functions of one-dimensional motion. The integrals in Eq. (13) and then in Eq. (11) are calculated numerically; the calculation is based on an expansion that includes the two lowest electron and hole levels ( $i$  and  $j$ ), at least ten Landau levels at  $B=12$  T, and up to 36 Landau levels at  $B=2$  T. An approximate technique of taking into account the nonparabolicity of heavy holes is described in Appendix to Ref. 9.

## 2.3. Interaction between excitons and FIR radiation

In the Faraday geometry (the wave vector of light is aligned with the magnetic field  $\mathbf{B}$ ), the Hamiltonian describing light absorption due to interaction between the excitons and FIR electric field with amplitude  $\mathcal{F}_0$  and frequency  $\omega$  has the form

$$\delta \hat{V}^\pm = \frac{e \mathcal{F}_0}{\omega} \left( \frac{\pi_e^\pm}{m_e} - \frac{\pi_h^\pm}{m_h} \right) \exp(-i\omega t). \quad (14)$$

Here the plus and minus signs denote left-handed (right-handed) circular polarization  $\sigma^\pm$ ;  $\pi_\alpha^\pm = \pi_{\alpha x} \pm i\pi_{\alpha y}$  ( $\alpha = e, h$ ), and

$$\pi_e = -i\hbar \nabla_e + \frac{e}{c} \mathbf{A}_e, \quad \pi_h = -i\hbar \nabla_h - \frac{e}{c} \mathbf{A}_h$$

are the kinematic momentum operators. One can show that

$$[\delta \hat{V}^\pm, \hat{\mathbf{K}}] = 0. \quad (15)$$

This means that the magnetic momentum does not change during an FIR transition. All populated exciton states contribute to intraband FIR transitions, including those with finite  $\mathbf{K}$ . This is the difference between intraband and interband transitions, since in the latter only excitons with  $\mathbf{K}=0$  are optically active. In this paper we consider only FIR transitions of excitons with center-of-mass momentum  $\mathbf{K}=0$ , which can be characterized by a constant angular momentum projection  $l_z$  (see Eq. (6)). Therefore, the selection rules for excitons with  $\mathbf{K}=0$  in a magnetic field  $B$  have the usual form

$$\langle \Psi'_{\mathbf{K}=0, l'_z} | \delta \hat{V}^\pm | \Psi_{\mathbf{K}=0, l_z} \rangle \sim \delta_{l'_z, l_z \pm 1}. \quad (16)$$

Effects related to FIR absorption by two-dimensional magnetoexcitons with  $\mathbf{K} \neq 0$  were discussed in Ref. 18b. By using expansion (9) and the formula

$$\delta \hat{V}^+ = \frac{i\sqrt{2}e\hbar \mathcal{F}_0}{\omega l_B} \left( \frac{a^\dagger}{m_e} - \frac{b}{m_h} \right) e^{-i\omega t}, \quad (17)$$

where  $a^\dagger$  ( $b^\dagger$ ) is the ladder operator corresponding to electron (hole) Landau levels (see Eq. (9)), we can express the matrix elements of intraband transitions between  $s$  and (for example)  $p^+$  exciton states by the formula

$$|f|^2 \sim |\langle \Psi_{\mathbf{K}=0, p^+} | \delta \hat{V}^+ | \Psi_{\mathbf{K}=0, s} \rangle|^2$$

$$\sim \left| \sum_{ij=1,2} \sum_n \sqrt{n+1} A_{ijn+1n}^* \left( \frac{A_{ijn} - A_{ijn+1n+1}}{m_e} - \frac{A_{ijn+1n+1}}{m_{h\parallel}} \right) \right|^2 I_B^{-2}. \quad (18)$$

For symmetric DQW (subscripts  $i, j = s, a$ ), FIR transitions in the Faraday geometry are allowed only between exciton states with the same spatial parity  $i \otimes j$  under inversion ( $z_e \rightarrow -z_e, z_h \rightarrow -z_h$ ):  $S \rightarrow S$  and  $A \rightarrow A$  (see also Sec. 2.4.1).

**2.4. Magnetoexcitons in DQW: qualitative description**

*2.4.1. Classification of states.* The DQW have four exciton terms (instead of one in an isolated quantum well when the lowest size-quantized level is taken into account).<sup>4,9,24,25</sup> The classification of the states depends on the  $R$ , which is the ratio between one-particle symmetric-antisymmetric  $e-h$  splitting  $\Delta_e, \Delta_h$  and the difference between the binding energies of direct ( $D$ ) and indirect ( $I$ ) excitons:  $\delta E_{ID} = E_D - E_I, R = \max(\Delta_e, \Delta_h) / \delta E_{DI}$ .

When  $R \ll 1$ , the wide-barrier regime of DQW is realized, and the exciton states in DQW are predominantly either direct or indirect.<sup>1</sup> In addition, there is splitting due to tunneling through the barrier: for example, in symmetric DQW at  $\mathcal{E} = 0$  each direct and indirect state is split into states symmetric ( $S$ ) and antisymmetric ( $A$ ) under inversion ( $z_e \rightarrow -z_e, z_h \rightarrow -z_h$ ). In the case of a wide barrier, the symmetric-antisymmetric splitting is governed by two-particle  $e-h$  tunneling through the barrier,  $\Delta_X \approx \Delta_e \Delta_h / \delta E_{DI}$ .<sup>9</sup> The splitting  $\Delta_X$  is suppressed by a rise in excitonic effects ( $\sim \delta E_{DI}^{-1}$ ); in particular, it decreases with increasing magnetic field  $B$ . In the wide-barrier regime, we will label exciton states by quantum numbers of the high magnetic field limit ( $D_{nm}, I_{nm}$ ) by indicating the numbers of  $e$  and  $h$  Landau levels that are dominant in expansion (9), and by the spatial character of the states. When necessary, we will indicate the state inversion symmetry ( $S$  or  $A$ ) at  $\mathcal{E} = 0$ , and under strong  $\mathcal{E}$  the lower ( $D_{nm}^-$  and  $I_{nm}^-$ ) and upper ( $D_{nm}^+$  and  $I_{nm}^+$ ) branches of the exciton spectrum (one example is shown in Fig. 2).

For a sufficiently thin barrier, the opposite limit is encountered,  $\Delta_e, \Delta_h \gg \delta E_{DI}$  and  $R \gg 1$ . In this regime, excitons cannot be classified as direct or indirect, since these states are mixed. Many of the characteristic features of the narrow-barrier regime can be understood in the one-particle approximation, neglecting excitonic effects.<sup>26,27</sup> Exciton states in symmetric DQW at  $\mathcal{E} = 0$  can be classified as  $ij_{nm}$ , where  $i, j = s, a$ , in accordance with the quantum numbers of electron and hole wave functions  $\zeta_i \xi_j \phi_{nm}$ , which dominate expansion (9). The states  $ss_{nm}$  and  $aa_{nm}$  ( $sa_{nm}$  and  $as_{nm}$ ) correspond to exciton states that are spatially symmetric  $S$  (antisymmetric  $A$ ).

*2.4.2. FIR transitions.* In a strong magnetic field, the exciton  $1s$  states are formed predominantly by the wave function  $\phi_{00}$  of the lowest  $e$  and  $h$  Landau levels. Owing to the Coulomb  $e-h$  interaction, there is a small admixture of states  $\phi_{nn}$  of higher Landau levels proportional to  $\sim I_B / a_{Be(h)} \ll 1$ , where  $a_{Be(h)} = \epsilon \hbar^2 / m_{e(h)} e^2$ . Similarly, the  $2p^+$  ( $2p^-$ ) exciton states are formed predominantly by the wave function  $\phi_{10}$  ( $\phi_{01}$ ) with a small admixture of

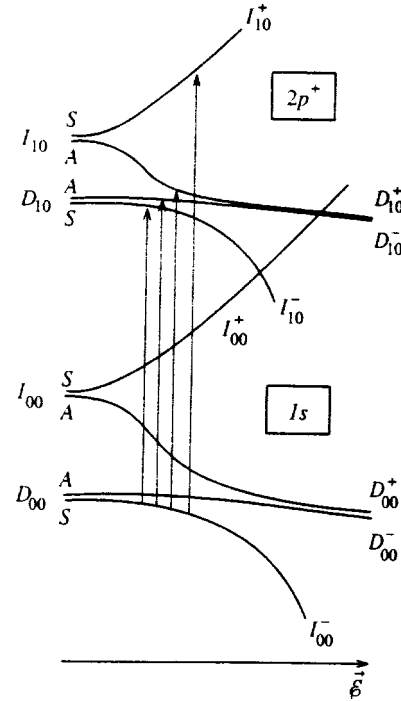


FIG. 2. Energies of  $1s$  and  $2p^+$  exciton states in DQW in the wide-barrier regime as functions of the electric field  $\mathcal{E}$ . Vertical arrows show the four lowest transitions from the  $1s$  ground state to  $2p^+$  excited states, depicted in detail in Fig. 4a.

$\phi_{n+1n}(\phi_{nn+1})$  states. Therefore the  $1s \rightarrow 2p^+$  ( $1s \rightarrow 2p^-$ ) excitation transition can be considered an electron (hole) cyclotron resonance,  $\phi_{00} \rightarrow \phi_{10}$  ( $\phi_{00} \rightarrow \phi_{01}$ ), which is modified by excitonic effects. The evolution of the energy and matrix elements of transitions from the symmetric  $1s$  ground states or  $D_{00}S$  to various  $p^\pm$  states in a magnetic field  $B$  at  $\mathcal{E} = 0$  in  $\text{In}_{0.2}\text{Ga}_{0.8}\text{As}/\text{GaAs}$  DQW were discussed in a previous publication.<sup>17</sup> For example, the strongest  $1s \rightarrow p^+$  transitions are  $D_{00}S \rightarrow D_{10}S$  and  $D_{00}S \rightarrow I_{10}S$ , i.e., the transition to the first electron Landau level. The transition energy is higher than the free-electron cyclotron energy, since the original  $1s$  state is more tightly bound than the final  $2p^\pm$  state. In DQW, the dipole matrix element  $|f^2|$  of the  $D_{00}S \rightarrow D_{10}S$  transition only increases with  $B$ . An explanation of such behavior was given in Ref. 17.

**3. NUMERICAL CALCULATIONS AND DISCUSSION**

In this part of the paper, we discuss results for symmetric  $\text{In}_{0.2}\text{Ga}_{0.8}\text{As}/\text{GaAs}$  DQW with  $L_1 = L_2 = 60 \text{ \AA}$ . Section 3.1 is dedicated to the dependence of energies and oscillator strengths of intraexciton FIR transitions on the barrier thickness  $L_b$  in a magnetic field  $B = 10 \text{ T}$  at  $\mathcal{E} = 0$ , and Secs. 3.2 and 3.3 to their dependence on the magnetic and electric fields at fixed  $L_b = 60 \text{ \AA}$ .

**3.1. Dependence on the barrier thickness**

An important parameter that determines many of the features of excitons in DQW (in particular, the character of a crossover from the direct to indirect regime in an applied electric field  $\mathcal{E}$ ) is the tunnel barrier thickness  $L_b$ , which

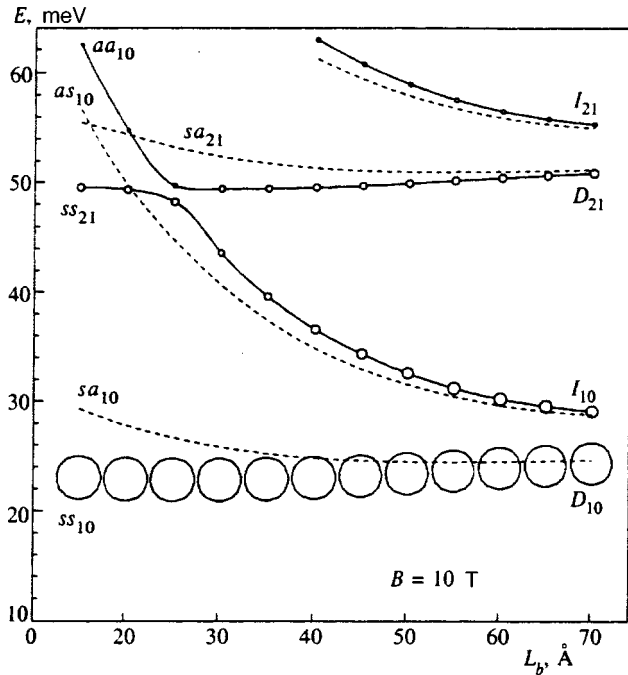


FIG. 3. Energies and dipole matrix elements of exciton transitions from the symmetric  $1s$  ground state to  $p^-$  excited states as functions of the barrier width  $L_b$  in an InGaAs/GaAs DQW with  $L_1=L_2=60$  Å and  $x=0.2$  at  $\mathcal{E}=0$ . The areas of open circles are proportional to  $|f|^2$  in Eq. (18). Dashed lines correspond to forbidden ( $S \rightarrow A$ ) transitions to antisymmetric final states. Characteristics of final states are labeled in the graph.

determines the coupling between the quantum wells. Energies and matrix elements of transitions from the symmetric  $1s$  ground state to  $p^+$  states are plotted versus  $L_b$  in Fig. 3. In the narrow-barrier regime, the initial state is formed mostly of the  $\zeta_s \xi_s \phi_{00}$  wave function denoted by  $ss_{00}$  (see Sec. 2.4.1), and two possible symmetric  $2p^+$  final states are  $ss_{10}$  and  $aa_{10}$  with the wave function  $\zeta_s \xi_s \phi_{10}$  and  $\zeta_a \xi_a \phi_{10}$ , respectively. The energies of these two transitions are  $\hbar\omega_{ce} + \delta E_1$  and  $\hbar\omega_{ce} + \Delta_e + \Delta_h + \delta E_2$ , respectively. Here  $\delta E_i$  are the energy corrections due to the differences in the Coulomb binding energies of the  $1s$  and  $2p^+$  states, and  $\delta E_2 \ll \Delta_e + \Delta_h$  for small  $L_b$ . The matrix element of the  $ss_{00} \rightarrow ss_{10}$  transition is large, and that of the  $ss_{00} \rightarrow aa_{10}$  transition is very small (and is due to the admixture of the  $aa_{00}$  state to  $ss_{00}$  and  $ss_{10}$  to  $aa_{10}$ ). As  $\Delta_e + \Delta_h > \hbar\omega_{ce}$  in the narrow-barrier regime, an anticrossing between the  $3p^+$  and  $ss_{21}$  states takes place at  $L_b \approx 25$  Å, which leads to a redistribution of oscillator strengths between the transitions.

After the crossover to the wide-barrier regime, excitons become predominantly either direct ( $D$ ) or indirect ( $I$ ). For example, the ground  $1s$  state is the  $D_{00}S$  exciton with the wave function  $(\zeta_s \xi_s + \zeta_a \xi_a) \phi_{00} / \sqrt{2}$ , and the two  $2p^+$  final states are the direct  $D_{10}S$  and indirect  $I_{10}S$  excitons with the wave functions  $(\zeta_s \xi_s \pm \zeta_a \xi_s) \phi_{10} / \sqrt{2}$ . Figure 3 shows that the energy of the transition to the first  $2p^+$  excited state increases very slowly with  $L_b$  because the changes in the binding energies of the initial and final states cancel each other. The transition energy to the next  $2p^+$  state (with the wave function  $\zeta_a \xi_a \phi_{10}$  at small  $L_b$  and  $(\zeta_s \xi_s - \zeta_a \xi_a) \phi_{10} / \sqrt{2}$  at large  $L_b$ ) rapidly drops with  $L_b$ , since the symmetric-

antisymmetric splitting  $\Delta_\alpha$  exponentially drops with the barrier width  $L_b$ . In the wide-barrier regime the parameter  $\Delta_\alpha$  is determined by one-particle tunneling across the barrier:  $\Delta_\alpha \approx |E_\alpha| \exp(-\mathcal{S}_\alpha) / \pi$ , where  $\mathcal{S}_\alpha = \sqrt{2m_{\alpha z}} |E_\alpha| L_b / \hbar$  and  $E_\alpha$  is the energy of the level in a single quantum well.<sup>28</sup>

In the considered case of In<sub>0.2</sub>Ga<sub>0.8</sub>As/GaAs DQW with  $L_1=L_2=60$  Å and, for example,  $L_b \approx 60$  Å, the numerical calculation yields<sup>9</sup>  $\Delta_e \approx 4.9$  meV and  $\Delta_h \approx 0.6$  meV. For large  $L_b$  the two lowest transitions to the  $2p^+$  states are the transitions to the direct ( $D_{00}S \rightarrow D_{10}S$ ) and indirect ( $D_{00}S \rightarrow I_{10}S$ ) excitons with the energy difference between them  $\approx \delta E_{DI} = E_D - E_I$ . The separation from the optically forbidden transitions to  $A$ -states  $\approx \Delta_X \approx \Delta_e \Delta_h / \delta e_{DI}$ . The transitions to the next Landau levels,  $D_{00}S \rightarrow D_{21}S$  and  $D_{00}S \rightarrow I_{21}S$ , correspond to the final  $3p^+$  states, and their oscillator strengths are considerably smaller.

### 3.2. Evolution of FIR transitions in an electric field at $B \neq 0$

A perpendicular electric field  $\mathcal{E}$  breaks the symmetry under inversion  $z \rightarrow -z$  and allows all  $s \rightarrow p^\pm$  transitions in DQW. Exciton  $1s$  and  $2p^\pm$  levels in an electric field  $\mathcal{E}$  in the wide-barrier regime are shown in Fig. 2. In a weak electric field, all levels shift quadratically due to the Stark effect. In intermediate fields, depending on Landau level numbers  $nm$ , the crossover between direct and indirect exciton states occurs. Owing to the lower Coulomb energy, this crossover happens in weaker electric fields for the  $2p^+$  state than for the  $1s$  state. This effect can be seen in the FIR absorption spectra.

Let us consider evolution of transitions from the ground  $1s$  state to the excited  $p^\pm$  states in the electric field  $\mathcal{E}$  and fixed magnetic field (Fig. 4). The transition to the first excited  $2p^+$  state experiences a red shift, which saturates in strong electric fields  $\mathcal{E}$ . This shift is also a function of  $B$ : the higher the magnetic field, the larger the red shift. This shift is controlled by excitonic effects. Indeed, in a weak field  $\mathcal{E}$  both the initial  $D_{00}$  and final  $D_{10}$  states are direct excitons. In a strong electric field, they become the indirect magnetoexcitons  $I_{00}^-$  and  $I_{10}^-$  with lower binding energies. As a result, the exciton transition energy drops and approaches that of the cyclotron resonance of free carriers (these energies are marked by arrows in Fig. 4).

Note also the nonmonotonic dependence of the energy of transition to the third  $2p^+$  excited state (at  $\mathcal{E}=0$  this is the  $D_{00}S \rightarrow I_{10}A$  transition, which is strictly forbidden by symmetry selection rules). This nonmonotonic behavior is due to successive crossovers from the direct state to the indirect state, first for the initial state and then for the final state in the FIR transition. The first crossover (when the third excited  $2p^+$  state transforms from the indirect  $I_{10}A$  to direct  $D_{10}^+$  magnetoexciton) occurs in a lower field  $\mathcal{E}$ , when the initial state is predominantly a spatially direct exciton  $D_{00}$ . This explains both the growth in the oscillator strength and red shift due to the larger Stark effect for the  $2p^+$  state. Then the initial  $1s$  state undergoes a crossover from  $D_{00}S$  to  $I_{00}^-$ . As a result, we have the  $I_{00}^- \rightarrow D_{10}^+$  transition, which has an oscillator strength decreasing with the field strength and a shift

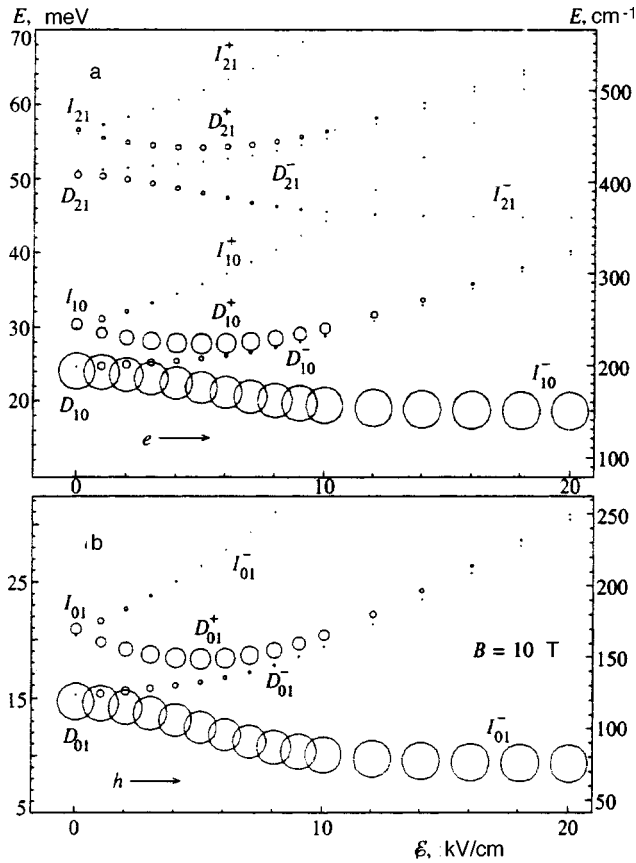


FIG. 4. Evolution in an electric field  $\mathcal{E}$  of energies and dipole matrix elements of transitions from the  $1s$  ground state to (a) excited  $p^+$  states and (b)  $p^-$  states in a magnetic field  $B=10$  T for symmetric InGaAs/GaAs DQW with  $L_1=L_2=60$  Å and  $x=0.2$ . The areas of open circles are proportional to the transition matrix element squared,  $|f|^2$ . The horizontal arrows indicate energies of cyclotron resonances for free electrons and holes. Characteristics of final states in the transitions are labeled in the graph.

almost linear in  $\mathcal{E}$  due to the Stark effect in the initial state  $I_{00}^-$  of the indirect exciton.

### 3.3. Evolution of FIR transitions in a magnetic field at fixed $\mathcal{E} \neq 0$

The binding energy of indirect excitons increases with  $B$  more slowly than that of direct excitons. Therefore a magnetic field  $B$  induces a crossover from an indirect to direct state in a strong fixed electric field  $\mathcal{E}$ , which depends on the Landau level numbers of the exciton states.<sup>4,9,25</sup> This effect can be seen in exciton FIR absorption spectra. The evolution of both the energies and dipole matrix elements of the  $1s \rightarrow p^+$  transition with the magnetic field  $B$  in the electric field  $\mathcal{E}=7$  kV/cm is illustrated by Fig. 5a, and in the field  $\mathcal{E}=17.2$  kV/cm by Fig. 5b.

In the stronger electric field  $\mathcal{E}$  (Fig. 5a), the initial  $1s$  state is the indirect exciton  $I_{00}^-$ . In the magnetic field range under consideration,  $B < 16$  T, no crossover between the direct and indirect states occurs, so only the  $I_{00}^- \rightarrow I_{10}^-$  transition has a large matrix element, which rapidly (essentially linearly) increases with  $B$ . Transitions to all remaining higher levels have much lower intensities.

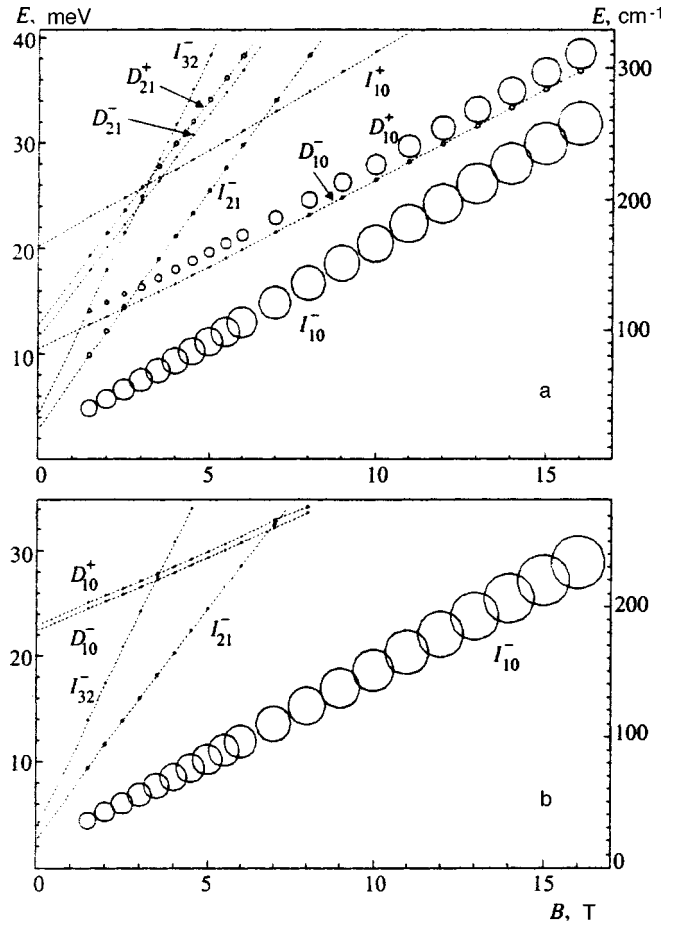


FIG. 5. Evolution in a magnetic field  $B$  of energies and dipole matrix elements of  $1s \rightarrow p^+$  transitions as functions of the magnetic field  $B$  in electric fields (a)  $\mathcal{E}=7$  kV/cm and (b)  $\mathcal{E}=17.2$  kV/cm. The dotted lines show positions of several weak transitions. The areas of open circles are proportional to dipole matrix elements squared,  $|f|^2$  [Eq. 18].

In the weaker electric field (Fig. 5b), the gap between the  $I_{10}^-$  and  $D_{10}^+$  states is considerably smaller. Furthermore, the mixing between direct and indirect exciton states is notable.<sup>9</sup> Therefore the  $I_{00}^- \rightarrow D_{10}^+$  transition has a notable matrix element even at intermediate magnetic fields  $B$ . At  $B < 4$  T, the behavior of spectral lines is complicated owing to numerous anticrossings between levels of direct  $np^+$  and indirect  $n'p^+$  excitons, where  $n' > n$ . This results in small splittings of lines and redistribution of their intensities, which is similar to the behavior of interband transitions discussed in Refs. 4 and 9. At  $B > 10$  T, the  $I_{00}^- \rightarrow D_{10}^+$  transition amplitude increases rapidly because of the indirect-to-direct crossover in the initial state: the ground state gradually evolves<sup>4,9</sup> and transforms from the indirect  $I_{00}^-$  to direct  $D_{00}^-$  exciton. Since the excitonic effects in  $2p^+$  states are considerably weaker, such a crossover occurs in much stronger magnetic fields.

Note that the transition to the final  $D_{10}^-$  state remains very weak because of the large difference between the shapes of wave functions of (almost degenerate)  $D_{10}^-$  and  $D_{10}^+$  direct excitons. Indeed, it follows from the probability distribution for the excitons (Fig. 6), i.e.,

$$P_{\mathbf{K}=0, l_z}(z_e, z_h) = \int d^2 \rho |\Psi_{\mathbf{K}=0, l_z}(\mathbf{r}_e, \mathbf{r}_h)|^2, \quad (19)$$

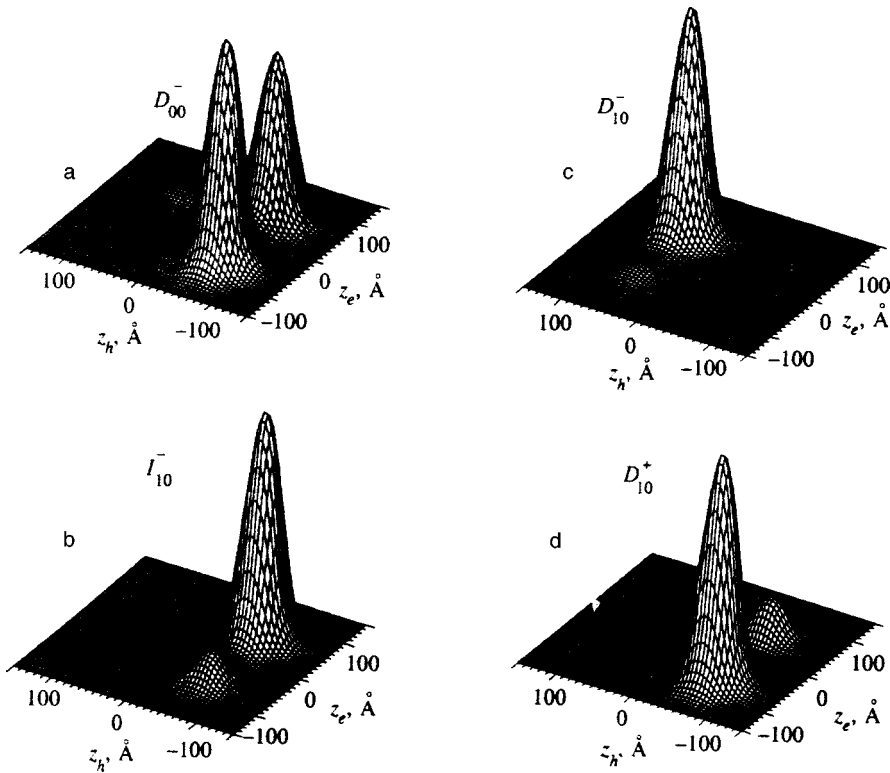


FIG. 6. Probability distributions  $P(z_e, z_h)$  (Eq. (19)) for exciton states involved in transitions shown in Fig. 5a ( $B=10$  T): a) initial  $1s$  state  $D_{00}^-$ ; three of the various low-lying  $2p^+$  final states: b)  $I_{10}^-$ , c)  $D_{10}^-$ , and d)  $D_{10}^+$ .

that in fields  $\mathcal{E}=7$  kV/cm and  $B=10$  T, the ground state at the lowest Landau levels (i.e., the initial state in the transitions in question) is predominantly direct (we denote it by  $D_{00}^-$ ). This state is predominantly a direct exciton in the left quantum well ( $z_e, z_h < 0$ ) with a large admixture of an indirect component ( $z_e < 0, z_h > 0$ ) and an extremely small component corresponding to a direct exciton in the right quantum well ( $z_e, z_h > 0$ ). In the same fields, the  $2p^+$  ground state is polarized because the Coulomb excitonic effects are not as strong, i.e., this is predominantly an indirect exciton  $I_{10}^-$  ( $z_e > 0, z_h < 0$ ) with a small admixture of the direct exciton ( $z_e, z_h < 0$ ). The dipole matrix element of the  $D_{00}^- \rightarrow I_{10}^-$  transition is large due to the large spatial overlap between the wave functions of these states. The next two excited  $2p^+$  states ( $D_{10}^-$  and  $D_{10}^+$ ) are predominantly direct excitons in the right and left quantum wells, respectively. As a result, only the  $D_{00}^- \rightarrow D_{10}^+$  transition is strong, whereas the  $D_{00}^- \rightarrow D_{10}^-$  transition is very weak because of the small spatial overlap between the wave functions of these two states.

#### 4. CONCLUSIONS

We have analyzed theoretically intraband magneto-optical transitions of direct and indirect excitons in InGaAs/GaAs coupled double quantum wells. Features in the behavior of transition energies and matrix elements due to the crossover from the narrow-barrier regime to the wide-barrier regime in an electric field  $\mathcal{E}$  and magnetic field  $B$  have been described. In particular, a red shift of the transition from the  $1s$  ground state to the first  $2p^+$  excited state in DQW due to the direct-indirect crossover in an electric field  $\mathcal{E}$  has been predicted. This effect is due to Coulomb excitonic effects

and increases with  $B$ . These theoretical results may be useful in planning experiments and interpreting their results.

The author is indebted to A. L. Yablonskii for designing computer codes used in numerical calculations, and to G. E. W. Bauer, L. V. Butov, A. A. Dremin, J. Kono, B. D. McCombe, and V. B. Timofeev for useful discussions. This work was supported by grants from Volkswagen, the Russian Fund for Fundamental Research, and INTAS.

\*E-mail: dzyub@gpi.ac.ru

<sup>1</sup>This classification is approximately applicable to the case of a barrier with an intermediate width, when  $R \sim 1$ . Note also that at a fixed  $L_b$  in sufficiently strong field  $B$  one can satisfy the condition  $R < 1$ .

<sup>1</sup>Y. Kuramoto and C. Horie, *Solid State Commun.* **25**, 713 (1978); I. V. Lerner, Yu. E. Lozovik, and D. R. Musin, *J. Phys. C* **14**, L311 (1980); D. Yoshioka and A. H. MacDonald, *J. Phys. Soc. Jpn.* **59**, 4211 (1990); X. M. Chen and J. J. Queen, *Phys. Rev. Lett.* **67**, 895 (1991).

<sup>2</sup>I. V. Lerner and Yu. E. Lozovik, *Zh. Eksp. Teor. Fiz.* **80**, 1488 (1981) [*Sov. Phys. JETP* **53**, 763 (1981)]; A. B. Dzyubenko and Yu. E. Lozovik, *Fiz. Tverd. Tela (Leningrad)* **25**, 1519 (1983); **26**, 1540 (1984) [*Sov. Phys. Solid State* **25**, 874 (1983); **26**, 938 (1984)].

<sup>3</sup>L. V. Butov, A. Zrenner, G. Abstreiter, G. Böhm, and G. Weimann, *Phys. Rev. Lett.* **73**, 304 (1994).

<sup>4</sup>L. V. Butov, A. Zrenner, G. Abstreiter, A. V. Petinova, and K. Eberl, *Phys. Rev. B* **52**, 12153 (1995).

<sup>5</sup>M. Bayer, V. B. Timofeev, F. Faller, T. Gutbrod, and A. Forchel, *Phys. Rev. B* **54**, 8799 (1996).

<sup>6</sup>J. Kono, B. D. McCombe, J.-P. Cheng, I. Lo, W. C. Mitchel, and C. E. Stutz, *Phys. Rev. B* **50**, 12492 (1994).

<sup>7</sup>J.-P. Cheng, J. Kono, B. D. McCombe, I. Lo, W. C. Mitchel, and C. E. Stutz, *Phys. Rev. Lett.* **74**, 450 (1995).

<sup>8</sup>L. V. Butov, in *Proceedings of the 23rd International Conference on Physics of Semiconductors (ICPS-23)*, M. Scheffler and R. Zimmermann (eds.), World Scientific, Singapore (1996), p. 1927.

<sup>9</sup>A. B. Dzyubenko and A. L. Yablonskii, *Phys. Rev. B* **53**, 16355 (1996).

- <sup>10</sup>D. Labrie, M. L. W. Thewalt, I. J. Booth, and G. Kirczenov, *Phys. Rev. Lett.* **61**, 1882 (1988).
- <sup>11</sup>C. C. Hodge, C. C. Phillips, M. S. Skolnick, G. W. Smith, C. R. Whitehouse, P. Dawson, and C. T. Foxon, *Phys. Rev. B* **41**, 12319 (1990).
- <sup>12</sup>M. Salib, H. A. Nickel, G. S. Herold, A. Petrou, B. D. McCombe, R. Chen, K. K. Bajaj, and W. Schaff, *Phys. Rev. Lett.* **77**, 1135 (1996).
- <sup>13</sup>J. Cerne, J. Kono, M. S. Sherwin, M. Sundaram, A. C. Gossard, and G. E. W. Bauer, *Phys. Rev. Lett.* **77**, 1131 (1996).
- <sup>14</sup>A. A. Dremin, V. B. Timofeev, D. Birkedal, and J. Hvam, *Phys. Status Solidi A* **164**, 557 (1997).
- <sup>15</sup>H. A. Nickel, G. H. Herold, M. S. Salib, G. Kioseoglou, A. Petrou, B. D. McCombe, and D. Broido, in *Proceedings of EP2DS-12*, Tokyo (1997), to be published in *Physica B*; J. Kono, M. Y. Su, J. Cerne, M. S. Sherwin, S. J. Allen Jr., T. Inoshita, T. Noda, and H. Sakaki, *ibid.*
- <sup>16</sup>J. Cen and K. K. Bajaj, *Phys. Rev. B* **47**, 1392 (1993).
- <sup>17</sup>A. B. Dzyubenko and A. L. Yablonskii, *JETP Lett.* **64**, 213 (1996).
- <sup>18</sup>a) A. B. Dzyubenko and A. L. Yablonskii, in *Proceedings of the 12th International Conference on High Magnetic Fields in the Physics of Semiconductors II*, G. Landwehr and W. Ossau (eds.), World Scientific, Singapore (1997), p. 693; b) A. B. Dzyubenko, *JETP Lett.* **66**, 617 (1997).
- <sup>19</sup>T. G. Andersson, Z. G. Chen, V. D. Kulakovskii, A. Uddin, J. T. Vallin, *Phys. Rev. B* **37**, 4032 (1988).
- <sup>20</sup>L. P. Gor'kov and I. E. Dzyaloshinskii, *Zh. Éksp. Teor. Fiz.* **53**, 717 (1967) [*Sov. Phys. JETP* **26**, 449 (1968)].
- <sup>21</sup>I. V. Lerner and Yu. E. Lozovik, *Zh. Éksp. Teor. Fiz.* **78**, 1167 (1980) [*Sov. Phys. JETP* **51**, 588 (1980)].
- <sup>22</sup>I. A. Malkin and V. I. Man'ko, *Zh. Éksp. Teor. Fiz.* **55**, 1014 (1968) [*Sov. Phys. JETP* **28**, 527 (1969)].
- <sup>23</sup>A. H. MacDonald and D. S. Ritchie, *Phys. Rev. B* **33**, 8336 (1986).
- <sup>24</sup>M. M. Dignam and J. E. Sipe, *Phys. Rev. B* **43**, 4084 (1991).
- <sup>25</sup>G. W. Bryant, *Phys. Rev. B* **46**, 1893 (1992).
- <sup>26</sup>Y. J. Chen, E. S. Koteles, B. S. Elman, and C. A. Armiento, *Phys. Rev. B* **36**, 4562 (1987).
- <sup>27</sup>S. Charbonneau, M. L. Thewalt, E. S. Koteles, and B. Elman, *Phys. Rev. B* **38**, 6287 (1988).
- <sup>28</sup>L. D. Landau and E. M. Lifshitz, *Quantum Mechanics. Nonrelativistic Theory*, Pergamon Press, New York (1976).

Translation was provided by the Russian Editorial office.